Available online at www.sciencedirect.com
SCIENCE DIRECT
Catalysis Today 101 (2005) 187–193
CATALYSIS TODAY
www.elsevier.com/locate/cattod

Photocatalytic degradation of herbicide fluroxypyr in aqueous suspension of TiO_2

M.A. Aramendía, A. Marinas *, J.M. Marinas, J.M. Moreno, F.J. Urbano

Departamento de Química Orgánica, Universidad de Córdoba, Edf. Marie Curie, Campus Universitario de Rabanales, 14014 Córdoba, Spain

Dedicated to Dr. J.C. del Amo, who died in the terrorist attack of March 11th 2004 in Madrid.

Abstract

The photocatalytic degradation of fluroxypyr (FLX) was studied using Degussa P-25 Titania as a catalyst. The disappearance of FLX was proved to follow a half-order kinetics. This implies that two active sites are involved in the adsorption of one molecule of fluroxypyr. In our conditions, complete mineralization of 40 ppm of pure fluroxypyr occurred within ca. 240 min of UV-radiation. Some reaction intermediates were identified by HPLC–MS (ESI+) and a tentative degradation pathway was proposed. The presence of HCl (pH 2) seemed to have an inhibiting effect on the initial rate, whereas degradation of FLX was accelerated at basic pH values (pH 8 or 10, achieved with $CaCO_3$ or NaOH, respectively). Photocatalysis proved to be an excellent new advanced oxidation technology (AOT) to eliminate fluroxypyr residues present in surface and ground waters.

Keywords: Fluroxypyr; Photocatalysis; Half-order kinetics; Photocatalytic degradation; Herbicide; Mineralization

1. Introduction

Fujishima and Honda [1] described, in 1972, the photocatalytic electrolysis of water using a titania electrode as anode and a platinum one as cathode. This discovery meant a milestone in photochemistry of semiconductors [2,3]. Nowadays, the following three are the main research areas dealing with this discipline: (i) hydrogen production through photoelectrochemical water electrolysis, as a continuation of Fujishima and Honda's pioneer research; (ii) photo-induced superhydrophilicity (PSH) [4,5] and (iii) heterogeneous photocatalysis involving mainly oxidation processes, such as photosterilization [6] and photomineralization [7], in a more general context referred to as photocatalytic oxidation (PCO). In this sense, heterogeneous photocatalysis (making use of solar light when possible [8]) has revealed as an efficient method for purifying water and air. Typical examples of water pollutants efficiently mineralized by photocatalysis are those coming from paper [9], dyes [10] and agrochemistry industries [8,11,12]. Regarding air pollution, VOCs and NO_x elimination can be cited [13–15].

The present piece of research deals with the photocatalytic oxidation (PCO) of fluroxypyr (4-amino-3,5-dichloro-6-fluoro-2-pyridinyl)oxyacetic acid, IUPAC name, FLX), a herbicide widely used in agriculture. Its structural formula is given in Fig. 1. It is used for control of a wide range of broadleaf weeds in sugar cane, cereals, sweetcorn and olive trees [16–19]. It is usually commercialized as an ester called starane (fluroxypyr-1-methylheptyl ester), which is rapidly degraded to fluroxypyr acid. Its oral LD_{50} in rats is above 5000 mg kg^{-1}. It is classified by EPA as Toxicity Category II and as ''not likely'' human carcinogen. However, subchronic toxicity assays in rats showed nephrotoxicity, increased kidney weight, hispathological lesions and decreased renal function [19].

This work must be seen in the context of a Project on Improvement of the Quality of Olive Oil carried out in our Department and supported by Junta de Andalucía. Such project involves, on the one hand, the detection and

* Corresponding author. Tel.: +34 957218622; fax: +34 957212066.
E-mail addresses: qo2maara@uco.es (A. Marinas), fj.urbano@uco.es (F.J. Urbano).

0920-5861/$ – see front matter © 2005 Elsevier B.V. All rights reserved.
doi:10.1016/j.cattod.2005.03.063

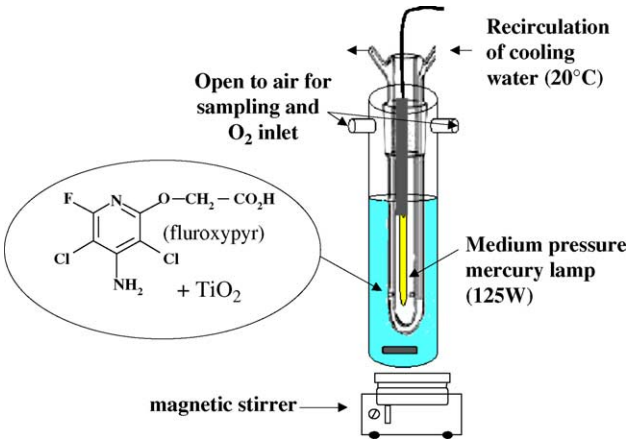

Fig. 1. Photocatalytic reactor and formula for fluroxypyr.

quantification of herbicide residues in olive oil (by GC–MS/MS) and on the other hand, the destruction of such residues in water by photocatalysis. Spain produces 34% of the total olive oil in the world, its olive groves being mainly concentrated in Andalucía.

2. Experimental

2.1. Chemicals

Pure fluroxypyr (99%, pestanal quality) was provided by Riedel de Häen. Ninety-six percent sulfuric acid, sodium nitrate, sodium nitrite, sodium chloride, ammonium fluoride, anhydrous sodium acetate, sodium hydroxide, 37% hydrochloric acid and L-(+)-tartaric acid were purchased from Panreac. Sodium carbonate and bicarbonate, 2,6-pyridinedicarboxylic acid (dipicolinic acid) and sodium and ammonium formate were provided by Sigma–Aldrich. Finally, formic acid was provided by Merck.

All photocatalytic degradation assays were carried out using titanium dioxide P-25 (mainly, anatase, ca. 50 $m^2\ g^{-1}$, non-porous) as photocatalyst. This catalyst was kindly provided by Degussa, Germany.

Water used for preparation of samples was Milli-Q quality water (Millipore Iberica, Spain).

2.2. Standard solutions

Fluroxypyr calibration was carried out from solutions of pure fluroxypyr in water in the range 0–40 mg L^{-1} ($r^2 = 0.9996$), analyzed by HPLC-UV. Solubility of fluroxypyr in water is ca. 90 mg L^{-1}.

Concerning anion detection, standard solutions containing $NaNO_3$ (nitrate determination), $NaNO_2$ (nitrite), NaCl (chloride), NH_4F (fluoride) and HCOONa (formic acid) in the range 0–10 mg L^{-1} were prepared. Regarding ammonium detection, $HCOONH_4$ solutions (0–10 mg L^{-1}) were utilized. In all cases, correlation coefficients obtained for calibration curves were over 0.99.

2.3. Photocatalysis experiments

All catalytic runs were performed in a Pyrex cylindrical double-walled immersion well reactor (23 cm long × 5 cm internal diameter, with a total volume of ca. 450 cm^3) open to air (Fig. 1). Irradiation of the reaction solutions was carried out by using a medium pressure 125 W Hg lamp (λ_{max} = 365 nm) supplied by Photochemical Reactors Ltd. (Model 3010). Lamp output was calculated to be ca. 1.5×10^{-3} Einstein/s (potassium ferrioxalate actinometry). Water used for cooling was thermostated at 20 °C.

Constant agitation of the suspension was insured by a magnetic stirrer placed at the reactor base.

Solutions of pure fluroxypyr were prepared in Milli-Q water and kept in the dark at 4 °C. Such solutions were never used for more than 5 days, despite the fact that samples seemed to be longer stable. Experiments were carried out from 200 mL of the mother solution and 50 mg of TiO_2. This TiO_2 amount was determined to be optimum to absorb all the incident photons. The mixture was maintained in the dark for 15 min under stirring to reach adsorption equilibrium, and was then irradiated. All degradation experiments were carried out at room temperature and with the photoreactor open to air. All experiments were performed at natural pH (ca. 4.0), unless otherwise stated, in particular for the study of pH influence.

2.4. Analyses

2.4.1. Kinetic studies

Samples taken at different times of irradiation were filtered through 0.22 μm, 25 mm ϕ nylon filters provided by Tracers, in order to remove TiO_2 particles before analyses by HPLC-UV at 210 nm (maximum of absorption for fluroxypyr). HPLC apparatus was a Spectra-System P2000 Liquid Chromatograph (Spectra Physics) equipped with an automatic injector (Spectra-System AS3000), a Spectra-100 UV–vis detector and a Tracer Kromasil 100 C18 column (150 mm × 2.1 mm i.d., 5 μm particle diameter). The composition of the binary mobile phase (flow rate 0.2 mL min^{-1}) was 40% acetonitrile and 60% H_2O (0.05% formic acid). Injection volume was 20 μL.

2.4.2. Mineralization studies

Evolution of inorganic ions (NO_3^-, NO_2^-, Cl^-, F^- and NH_4^+) together with $HCOO^-$ was followed by conductivity HPLC. Quantification was possible using the corresponding calibration curves. CH_3COO^- was also detected. However, it appeared as a shoulder of the peak obtained for F^-, which did not allow its precise quantification. The HPLC system used comprised a Metrohm Metrosep anion dual two column (75 mm × 4.6 mm i.d., 5 μm particle diameter), a Metrohm 753 ionic suppression module (using H_2SO_4 for regeneration of cartridges) and a Metrohm 732 ionic conductivity detector. Mobile phase was a mixture of Na_2CO_3 (1.3 mmol L^{-1}) and $NaHCO_3$ (2.0 mmol L^{-1}), flow rate 0.8 mL min^{-1}. Injection volume was 20 μL.

For ammonium ion determination, ion suppresion module was not necessary and a Metrohm Metrosep C2 100 column (100 mm × 4.0 mm i.d., 5 μm particle diameter) was used. Mobile phase was a mixture of dipicolinic acid (0.75 mmol L^{-1}) and L-(+)-tartaric acid (4 mmol L^{-1}), flow rate 1 mL min^{-1}. Injection volume was 10 μL.

For total organic carbon (TOC) analyses, a Rosemount analytical Dohrmann DC-190 carbon analyzer was used. A standard solution of potassium phthalate was used for calibration.

Moreover, a VG Sensorlab quadrupole Mass Spectrometer was connected online to the reactor in order to monitor CO_2 evolution during photocatalytical process. It was operated in the multiple ion-monitoring (MIM) mode. Selected peaks were $m/z = 44$ and 28.

2.4.3. By-product evaluation

HPLC–MS analyses were performed at the Mass Spectrometry Service of the University of Cordoba, on a triple–quadrupole LC–MS equipment (Varian LC–MS 1200 L). Positive electrospray (capillary voltage of 4.0 kV) was used for ionization of analytes. The drying gas temperature (N_2) was 250 °C and the detector voltage 1800 V. Source current: 5 μA. Capillary voltage: 40 V. Mass range: 100–350 a.m.u. HPLC conditions were the same as for HPLC-UV experiments.

3. Results and discussion

3.1. Kinetics of fluroxypyr disappearance

Fig. 2 shows a typical degradation kinetic curve. Results found for degradation in the absence of catalyst (direct photolysis) are there depicted, together with those obtained for the photocatalytic process (UV light + catalyst). Error bars indicate the standard deviation (S.D.). Experiments were performed three times and the points correspond to the average of the repetitions. As can be seen, FLX disappearance is quite fast (around 60 min) in our conditions, the initial rate being 3.52 ppm min^{-1}. The fact that the reaction volume was 200 mL allowed us to sample 10 times at each experience (2 mL each), thus avoiding significant mistakes due to the sampling of an excessive volume (volume variation ca. 10%). Other experiments were made in which the initial concentration of the herbicide was varied to determine the partial order with respect to fluroxypyr. Initially, the disappearance of FLX was estimated to be of the apparent first order, as already observed for many herbicides and in agreement with a Langmuir–Hinshelwood kinetic formation [20,21]. However, when varying the initial concentration C_0, there resulted that the first-order rate constant did not remain constant. This reminded us of a previous work [12], which showed that the photocatalytic disappearance of an insecticide–acaricide called formetanate followed a half-order kinetics. This would imply that two active sites are involved in the adsorption of one molecule of FLX. Such a half-order kinetics has also been observed for photocatalytic degradation of certain sulfonylurea herbicides in TiO_2 aqueous suspension [22], the interaction of HCOOH and TiO_2-supported Pt [23] or the gas-phase photocatalytic oxidation of ethanol on titania [24].

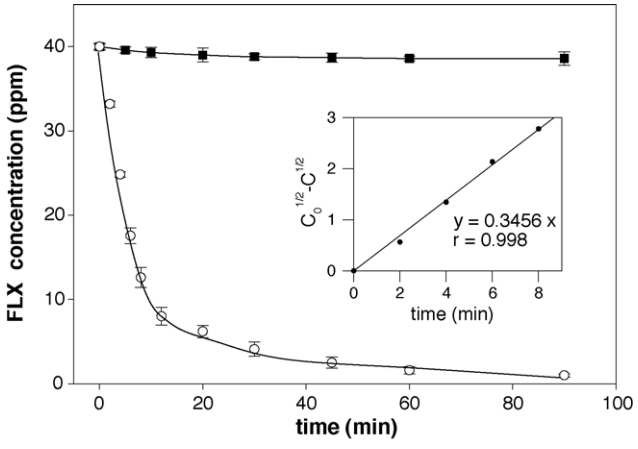

Fig. 2. Direct photolysis (full squares) and photocatalytic degradation of fluroxypyr. Error bars indicate the standard deviation. The inset shows the linear transform of the integrated half-order kinetics.

When two active sites in the catalyst are involved in adsorption, the coverage θ can be expressed as:

$$\theta = \frac{(KC)^{1/2}}{1 + (KC)^{1/2}} \quad (1)$$

On the other hand, $r = k\theta$ (Langmuir–Hinselwood expression of the rate).

At high dilutions, $(KC)^{1/2} \ll 1$, thus getting:

$$r = k\theta = k\left[\frac{(KC)^{1/2}}{1 + (KC)^{1/2}}\right] \approx k(KC)^{1/2} = k_{app}C^{1/2} \quad (2)$$

where k_{app} denotes the apparent rate constant.

Integrating this expression between $t = 0$ (C_0) and t (C), one gets:

$$r = -\frac{dC}{dt} = k_{app}C^{1/2} \Rightarrow [C_0^{1/2} - C^{1/2}] = \frac{k_{app}}{2}t \quad (3)$$

Therefore, according to Eq. (3) if we plot $[C_0^{1/2} - C^{1/2}]$ against t, a line should be obtained. This is consistent with results shown in the inset of Fig. 2. Moreover, from Eq. (2), if we plot log r_0 (i.e., the initial rate) as a function of log C_0, a linear diagram with the slope being close to =0.5 should be obtained. Results depicted in Fig. 3a confirm our hypothesis. Furthermore, a tentative explanation for the adsorption of FLX on TiO_2 is given in Fig. 3b.

Looking at the formula of FLX (Fig. 1) there are three groups, which could potentially interact with active sites in the catalyst: the carboxylic group and both nitrogen groups. FLX is an acid with a pK_a 2.2 [25]. Its natural pH (i.e., pH of

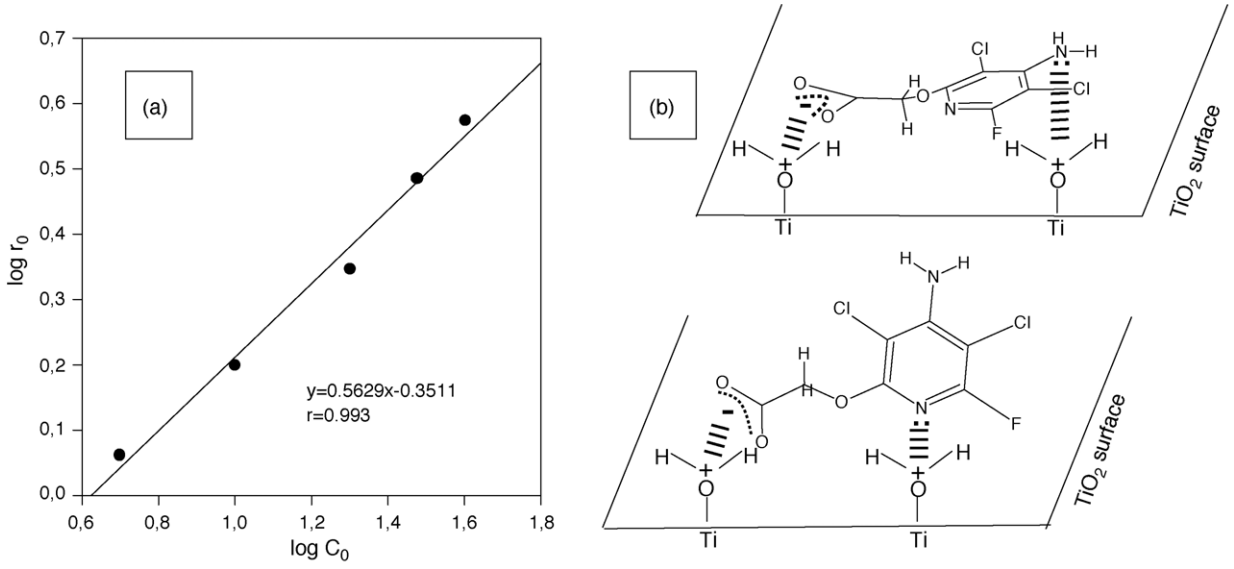

Fig. 3. Kinetic study of fluroxypyr disappearance at five different initial concentrations: (a) evidence for a half-order kinetics with respect to fluroxypyr concentration indicative of the involvement of two active sites in the adsorption; (b) suggested interactions between active sites on titania surface and fluroxypyr.

a 40 ppm FLX aqueous solution) was measured to be 4.0. Therefore, if we denote FLX as RCOOH:

$$k_a = \frac{[\mathrm{RCOO^-}][\mathrm{H^+}]}{[\mathrm{RCOOH}]} \Rightarrow \mathrm{pH} - \mathrm{p}K_\mathrm{a}$$

$$1.8 = \log \frac{[\mathrm{RCOO^-}]}{[\mathrm{RCOOH}]} \Rightarrow \frac{[\mathrm{RCOO^-}]}{[\mathrm{RCOOH}]} \approx 63$$

It means that in our aqueous solution, there are ca. 63 molecules of FLX in their anionic form per molecule in its neutral form. On the other hand, the point zero charge (PZC) for TiO_2 Degussa P25 is known to be around 6.3 [26,27]. Therefore at pH < 6.3, as it is the case (pH 4.0), titania surface will be positively charged ($TiOH_2^+$). Consequently, one of the two adsorption sites implied in the adsorption could involve a $RCOO^-/TiO_2H^+$ interaction (i.e., electrostatic attraction between carboxylate molecules, predominant in solution, and positively charged catalyst surface). As for the other group in FLX molecule involved in the adsorption, on the one hand, one could think of nitrogen in the pyridine group since its basicity is higher than that of the other primary amino group. On the other hand, results found by Poulios et al. [28] for photocatalytic degradation of another pyridine herbicide called triclopyr (3,5,6-trichloro-2-pyridinyloxyacetic acid, pK_a=2.93) over aqueous suspension of TiO_2, seem to suggest an interaction through the primary amino group. Triclopyr degradation followed a first-order kinetics, the authors suggesting only an interaction through the carboxylate group. In any case, this requires further studies. Infrared spectroscopy studies are currently being made which could confirm the interaction between catalyst sites and FLX molecules through carboxylate species [28,29] and amino groups [30] as well as whether adsorption of aromatic ring in FLX is flat or not [31].

3.2. Mineralization evaluation

A complete degradation of an organic molecule by photocatalysis normally leads to gaseous CO_2, and the heteroatoms turn into inorganic anions that remain in solution. Looking at the formula for fluroxypyr (Fig. 1), one can expect the formation of NO_2^-, NO_3^- and/or NH_4^+ (regarding nitrogen content in the molecule) as well as F^- and Cl^-. The overall equation, valid after long irradiation time in the presence of excess oxygen, which describes photocatalytic mineralization of FLX is presented below:

$$\mathrm{C_7H_5O_3N_2Cl_2F} + \tfrac{17}{2}\mathrm{O_2} \rightarrow \text{intermediates} \rightarrow 7\mathrm{CO_2} + 2\mathrm{NO_3^-} + 2\mathrm{Cl^-} + \mathrm{F^-} + 5\mathrm{H^+}$$

Fig. 4 shows the evolution profile for inorganic ions. As far as nitrogen evolution is concerned, 93% of nitrogen in FLX is converted into ammonium (major species), nitrate and nitrite in about 4 h of irradiation. Nitrite is present as traces reaching a maximum at about 20 min of irradiation. It is probably a moment when the amount of dissolved oxygen is not enough for complete oxidation of all species. This punctual lack of oxygen coincides with the maximum in CO_2 formation as mentioned below. Oxidation of ammonium to nitrate will probably take longer [32]. Regarding both fluorine and chlorine atoms in FLX, they are converted into fluoride and chloride species, respectively, within ca. 60 min of irradiation (conversion over 90%). The fact that generation of Cl^- and F^- is faster than that of nitrogenated species suggests a mechanism through direct substitution of Cl and F atoms by OH radicals. In contrast, mineralization of pyridynic nitrogen would require a previous ring-opening, thus taking longer. This is consistent with results reported in the literature [32].

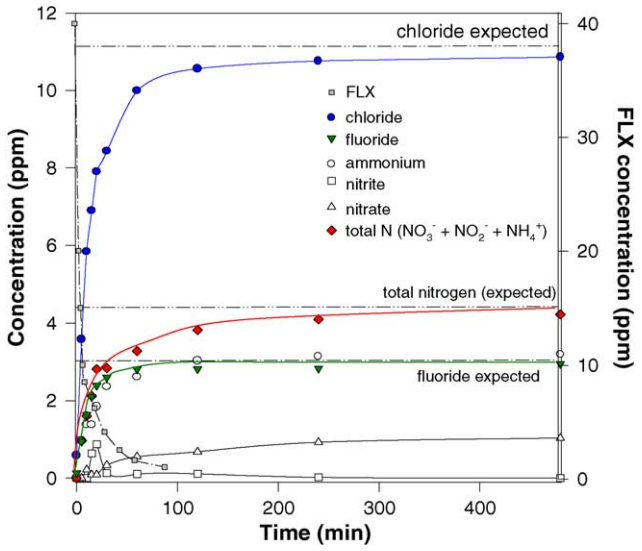

Fig. 4. Evolution of nitrogen (ammonium, nitrate, nitrite and total), fluoride and chloride species during the degradation of fluroxypyr (C_0 = 40 ppm).

As for CO_2 evolution (Fig. 5), over 90% of the carbon atoms were transformed into CO_2 after ca. 240 min of treatment, the maximum of CO_2 generation (as detected by MS) occurring at ca. 20 min of irradiation. It is also the irradiation time for which maximum concentration of formate and nitrite species was detected which supports the hypothesis that a punctual lack of dissolved oxygen occurs at that moment.

3.3. Intermediates

A solution sample corresponding to fluroxypyr irradiated for 20 min was analyzed by HPLC–MS (ESI+). This is the time at which maximum concentrations of primary intermediates were observed by HPLC-UV. Detected intermediates together with the tentative degradation pathway are shown in Fig. 6. It is well established that the

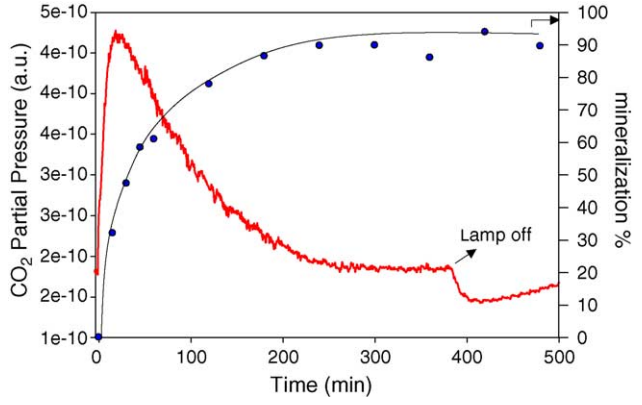

Fig. 5. CO_2 evolution during photocatalytic degradation of fluroxypyr (C_0 = 40 ppm) online monitored by MS and determined by TOC measurements.

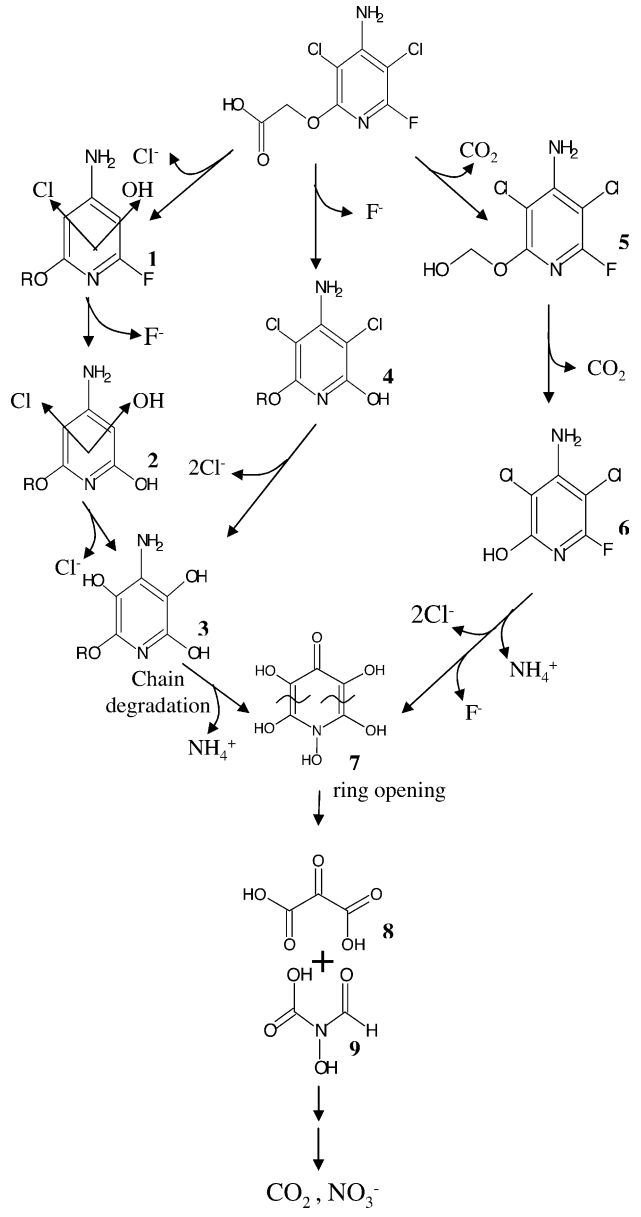

Fig. 6. Fluroxypyr photocatalytic degradation: some intermediates detected by HPLC–MS (ESI+) together with the corresponding tentative degradation pathway. Hydroxyl radicals have been omitted in the scheme.

irradiation of an aqueous TiO_2 suspension with light energy equal or greater than that of the band gap ($E_g \geq 3.2$ eV) leads to the generation of holes (h^+) and electrons (e^-) in the valence and conduction bands, respectively.

$$TiO_2 + h\nu \rightarrow e^- + h^+$$

Degradation of the organic pollutant may occur directly by holes or indirectly by hydroxyl radicals generated from such holes:

$$h^+ + H_2O \rightarrow OH^\bullet + H^+$$
$$h^+ + OH^- \rightarrow OH^\bullet$$
$$D + OH^\bullet \rightarrow \text{indirect oxidation}$$
$$D + h^+ \rightarrow \text{direct oxidation}$$

where "D" denotes an electron donor (i.e., the organic pollutant).

As far as the electron in the conduction band is concerned, it usually reduces oxygen according to:

$$e^- + O_2 \rightarrow O_2^-$$

In our case, the proposed mechanism would involve a non-selective hydroxylation of the aromatic ring (Cl and F atoms, being substituted by an OH group) and a degradation of the side chain. Compounds **1, 2** and **4** are evidence for the former, whereas **5** and **6** are indicative of the latter. It is worthy noting that initial rate of appearance of chloride species (0.011 mol L^{-1} min^{-1}) is ca. twice the value of fluorine one (0.006 mol L^{-1} min^{-1}). As Cl/F ratio in FLX is 2, it means that hydroxyl radicals generated in photocatalytic process have a similar efficiency in the cleavage of C–F and C–Cl bonds. Their high oxidation potential (E^0 = 2.8 V) can account for that.

Photocatalytic degradation of the side chain will probably start by the so-called Photo-Kolbe process [33] according to which:

$$RCOO^- + h^+ \rightarrow R^\bullet + CO_2$$

where h^+ denotes a photohole.

Subsequently, progressive oxidation of resulting radical to alcohol (compound **5**), aldehyde and finally to carboxylic acid would lead to a new Photo-Kolbe reaction, thus resulting in the final substitution of the chain by a hydroxyl group (see intermediate labeled as **6**). Formation of ammonium (from intermediate **3–7**) could occur via hydrolysis of an imine as described by Piccinini et al. [34]. In order to simplify Fig. 6, such an intermediate has not been included there. As far as the ring-opening is concerned, it would take place by the C–C bond in diols generated by hydroxyl attack on two neighbour positions as described elsewhere for 3-amino-2-chloropyridine [32] or aminopyrimidines [35]. In the case of intermediate **7**, ring-opening would yield compounds **8** and **9**.

3.4. Influence of pH

Three experiments were performed varying the initial pH of the 40 ppm FLX solution through the addition of HCl (up to pH 2), NaOH (pH 10) and $CaCO_3$ (pH 8). The addition of such chemicals will have two main effects on photocatalytical process. Firstly, inorganic ions can compete with organic compounds for active sites in the catalyst as well as influence redox processes according to their oxidation potentials [36]. Secondly, the change in pH may provoke a change in adsorption degree though a modification in the ionization state of titania surface [37,38]. Results found for the three above-mentioned cases were compared to that obtained for a 40 ppm FLX aqueous solution (natural pH 4). Initial rate of disappearance for FLX decreased considerably in the presence of HCl (from 3.52 ppm min^{-1} at natural pH to ca. 2.30 ppm min^{-1}). This is probably due to (i) the presence of chlorine species which are known to compete with organic compounds for the photogenerated oxidative species [36] and (ii) the existence of a lesser amount of fluroxypyr as carboxylate (note that pK_a = 2.2). On the contrary, the increase in pH leads to an increase in reaction rate passing from 3.52 (natural pH, pH 4) to 5.57 ppm min^{-1} ($CaCO_3$, pH 8) or 5.01 ppm min^{-1} (NaOH, pH 10). In these two cases, there are two factors to take into account. On the one hand, the higher the pH, the lower FLX adsorption due to electrostatic repulsion between the negatively-charged titania surface and FLX in its carboxylate form. On the other hand, the higher the pH value, the higher the number of hydroxyl ions in solution. Since more hydroxyl radicals can be formed by trapping photoproduced surfacial electron holes by hydroxyl anions ($OH^- + h^+ \rightarrow OH^\bullet$), reaction rate increases [38,39]. It seems that this second factor is more crucial, thus accounting for the observed increase in reaction rate.

Fluroxypyr did not undergo significant direct photolysis at pH 8 (achieved with $CaCO_3$) or pH 10 (NaOH). Moreover, in a previous study [12] we showed that $CaCO_3$ had no inhibiting effect on photocatalytic experiments.

The fact that the kinetics is increased by dissolved limestone is of particular interest, since it reproduces the conditions found in ground waters, mainly those of Almería.

4. Conclusions

The above-mentioned results allow us to draw the following conclusions.

Photocatalytic degradation of FLX in a titania aqueous suspension has been studied. In our conditions, complete mineralization of FLX was achieved within ca. 240 min of UV-radiation. Disappearance of FLX followed a half-order kinetics, indicative of the involvement of two active sites in the adsorption. The mechanism suggested for photocatalytic degradation of fluroxypyr involves a non-selective hydroxylation of the aromatic ring (Cl and F atoms being substituted by an OH group) and a degradation of the side chain. As far as the ring-opening is concerned, it would take place by the C–C bonds in diols generated by hydroxyl attack on two neighbor positions. The presence of HCl (pH 2) had an inhibiting effect on the initial rate, probably due to the competition of chlorine and organic pollutant for oxygen. On the contrary, NaOH (pH 10) and $CaCO_3$ (pH 8) led to a quicker degradation of FLX. The existence of more hydroxyl anions, which can lead to hydroxyl radicals ($OH^- + h^+ \rightarrow OH^\bullet$) might account for that.

Acknowledgments

The authors gratefully acknowledge the financial support from Junta de Andalucía (CAO00-005) and Ministerio de Ciencia y Tecnología in the framework of Projects

BQU2001-2605 and CTQ2004-02200 (co-financed with FEDER funds). Prof. A. Martín and Dr. M.A. Martín are also thanked for TOC measurements. A. Marinas is thankful to Junta de Andalucía for a contract. Finally, the authors are grateful to Dr. Lafont from SCAI of Cordoba University for HPLC–MS experiments.

References

[1] A. Fujishima, K. Honda, Nature 37 (1972) 238.
[2] A. Fujishima, T.N. Rao, D.A. Tryk, J. Photochem. Photobiol. C 1 (2000) 1.
[3] A. Mills, S.K. Lee, J. Photochem. Photobiol. A 152 (2002) 233.
[4] P. Gould, Mater. Today 6 (2003) 44.
[5] Y. Gao, Y. Masuda, K. Koumoto, Langmuir 20 (2004) 3188.
[6] H. Tamai, N. Katsu, K. Ono, H. Yasuda, J. Mater. Sci. 37 (2002) 3175.
[7] P. Pichat, in: M.A. Tarr (Ed.), Chemical Degradation Methods for Wastes and Pollutants: Environmental and Industrial Applications, Marcel Dekker Inc., New York, Basel, 2003, pp. 77–119.
[8] S. Malato, J. Blanco, A. Vidal, D. Alarcón, M.I. Maldonado, J. Cáceres, W. Gernjak, Solar Energy 75 (2003) 329.
[9] A.M. Peiró, J.A. Ayllón, J. Peral, X. Doménech, Appl. Catal. B 30 (2001) 359.
[10] C. Guillard, J. Disdier, C. Monnet, J. Dussaud, S. Malato, J. Blanco, M.I. Maldonado, J.-M. Herrmann, Appl. Catal. B 46 (2003) 319.
[11] H.D. Burrows, M. Canle L, J.A. Santaballa, S. Steenken, J. Photochem. Photobiol. B 67 (2002) 71.
[12] A. Marinas, C. Guillard, J.M. Marinas, A. Fernández-Alba, J.-M. Herrmann, Appl. Catal. B 34 (2001) 241.
[13] M. Lewandowski, D.F. Ollis, in: V. Ramamurthy, K.S. Schanze (Eds.), Semiconductor Photochemistry and Photophysics, Marcel Dekker Inc., New York, Basel, 2004, pp. 249–282.
[14] X. Fu, W.A. Zeltner, M.A. Anderson, in: P.V. Kamat, D. Meisel (Eds.), Semiconductor Nanoclusters, Elsevier, Amsterdam, 1996, pp. 445–461.
[15] S.O. Hay, T.N. Obee, Adv. Oxid. Technol. 4 (1999) 209.
[16] K. Domaradzki, J. Plant Protec. Res. 43 (2003) 247.
[17] K.J. Kirkland, E.N. Johnson, F.C. Stevenson, Weed Technol. 15 (2001) 48.
[18] N.N. Vettakkorumakankav, S. Deshpande, T.A. Walsh, J.C. Hall, Weed Sci. 50 (2002) 713.
[19] EPA Fluroxypyr Fact sheet available at http://www.epa.gov/opprd001/factsheets/fluroxypyr.pdf.
[20] P. Pichat, J.M. Herrmann, in: N. Serpone, E. Pelizzetti (Eds.), Photocatalysis: Fundamentals and Applications, John Wiley and Sons, 1989 pp. 217–250.
[21] C.S. Turchi, D.F. Ollis, J. Catal. 122 (1990) 178.
[22] E. Vulliet, J.-M. Chovelon, C. Guillard, J.-M. Herrmann, J. Photochem. Photobiol. A 159 (2003) 71.
[23] J. Raskó, T. Kecskés, J. Kiss, J. Catal. 224 (2004) 261.
[24] E. Piera, J.A. Ayllón, X. Doménech, J. Peral, Catal. Today 76 (2002) 259.
[25] Data taken from Scifinder Scholar, American Chemical Society, calculated using Advanced Chemistry Development (ACD) SoftwareSolaris V4.67, 2001.
[26] J.A. Navío, J.J. Testa, P. Djedjeian, J.R. Padrón, D. Rodríguez, M.I. Litter, Appl. Catal. A 178 (1999) 199.
[27] D.N. Furlong, D. Wells, W.H.F. Sasse, J. Phys. Chem. 89 (1985) 626.
[28] I. Poulios, M. Kositzi, A. Kouras, J. Photochem. Photobiol. A 115 (1998) 175.
[29] A. Piscopo, D. Robert, J.V. Weber, Appl. Catal. B 35 (2001) 117.
[30] J. Araña, J.M. Rodríguez, E. Tello Rendón, C. Garriga, I. Cabo, O. González Díaz, J.A. Herrera-Melián, J. Pérez-Peña, G. Colón, J.A. Navío, Appl. Catal. B 44 (2003) 153.
[31] D. Ferri, T. Bürgi, A. Baiker, J. Catal. 210 (2002) 160.
[32] B.F. Abramović, V.B. Anderluh, A.S. Topalov, F.F. Gaál, Appl. Catal. B 48 (2004) 213.
[33] B. Kraeutler, A.J. Bard, J. Am. Chem. Soc. 99 (1977) 7729.
[34] P. Piccinini, C. Minero, M. Vincenti, E. Pelizzetti, Catal. Today 39 (1997) 187.
[35] P. Calza, C. Medana, C. Baiocchi, E. Pelizzettti, Appl. Catal. B 52 (2004) 267.
[36] P. Calza, E. Pelizzetti, Pure Appl. Chem. 73 (2001) 1839.
[37] G. Low, S. McEvoy, R. Matthews, Environ. Sci. Technol. 25 (1991) 460.
[38] D. Bahnemann, J. Cunningham, M.A. Fox, E. Pelizzetti, P. Pichat, N. Serpone, in: G.R. Helz, R.G. Zepp, D.G. Crosby (Eds.), Aquatic and Surface Photochemistry, Lewis Publ., Boca Raton, FL, 1994 pp. 261–316.
[39] S. Tanaka, U.K. Saha, Water Sci. Technol. 30 (1994) 47.